Insights into the effect of oxygen functional groups on the heterogeneous electron transfer at activated carbons from scanning electrochemical microscopy

Giovanna Franklin, El-Mahdi Halim, Céline Merlet, Pierre-Louis Taberna, Patrice Simon

– Insights into the effect of oxygen functional groups on the heterogeneous electron transfer at activated carbons from scanning electrochemical microscopy

Giovanna Franklin[1,2], El-Mahdi Halim[1], Celine Merlet[1,2], Pierre-Louis Taberna[1,2*], Patrice Simon[1,2]

CIRIMAT, Université Toulouse 3 Paul Sabatier, Toulouse INP, CNRS, Université de Toulouse, 118 Route de Narbonne, 31062 Toulouse cedex 9 - France

Réseau sur le Stockage Electrochimique de l'Énergie (RS2E), Fédération de Recherche CNRS 3459, 80039 Amiens, France.

Corresponding Author e-mail : Pierre-Louis Taberna (pierre-louis.taberna@univ-tlse3.fr)

Abstract

The influence of surface chemistry on heterogeneous electron transfer at activated carbon (AC) electrodes was studied using scanning electrochemical microscopy (SECM) and conventional electrochemical measurements, which allow for measuring respectively the local and the overall electrode electron transfer rate constants. Using a thermal treatment in air and under argon, commercial activated carbons were either oxidized or defunctionalized. Both treatments lead to a slight decrease of the specific surface area of the material, without altering its pore size distribution and morphology. The nanogap voltammetry and approach curves obtained by SECM were used to characterize the rate constants at the interface between an aqueous solution of ferrocenemethanol (FcMeOH) and the AC electrodes. The heterogeneous electron transfer (HET) rate constant for the untreated AC was $3.4\ 10^{-2} \pm 0.2$ cm s^{-1} and was increased by about 2.5 and 1.5 times, after oxidizing and defunctionalizing the surface, respectively. SECM results showed that the heat treatment increases the conductivity of AC, and the oxidation of the surface increases the wettability and accessibility of the pores, which are assumed to promote the electron transfer. The local heterogeneous electron transfer rate constant values obtained by SECM are higher, by an order of magnitude, than the global ones obtained from conventional electrochemical macroelectrode measurements. The local information obtained by SECM is valuable for understanding the nanoscale interfacial mechanisms in porous carbon electrodes as a better understanding of the charge storage mechanism is key to improve their electrochemical performances.

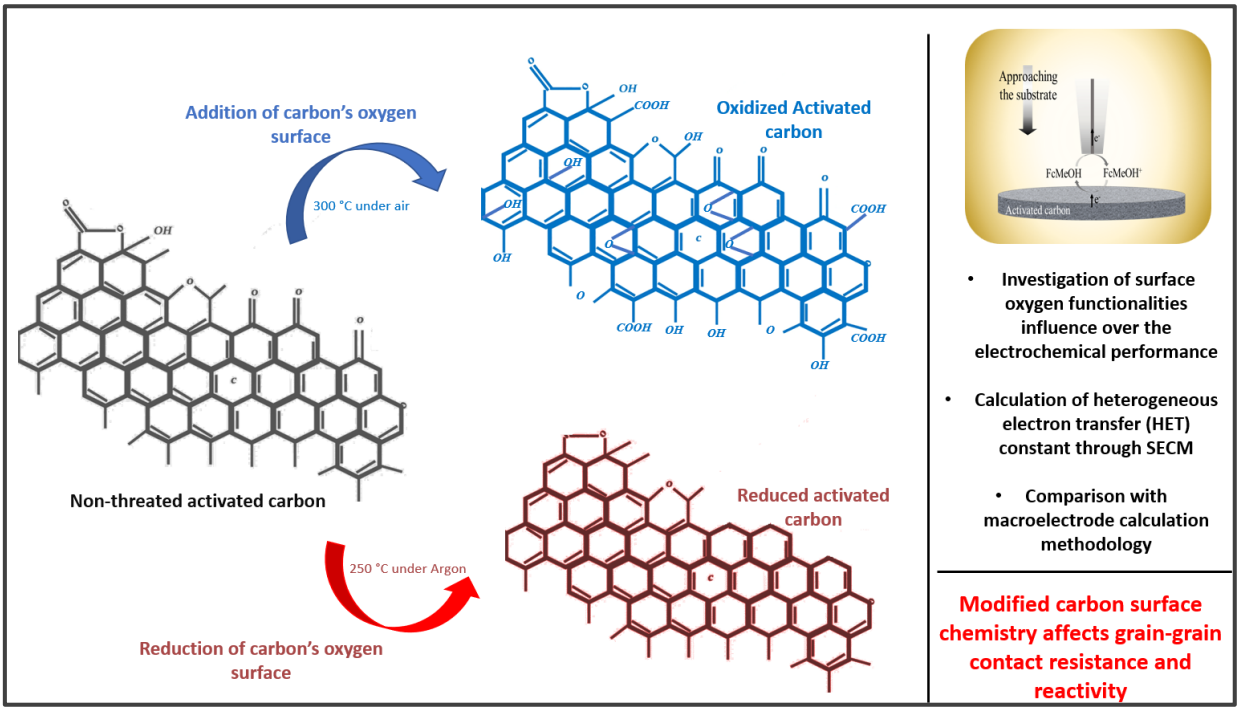

Keywords:, Scanning electrochemical microscopy, Activated carbon, heterogeneous electron transfer rate constant, surface oxygen groups influence

Introduction

The massive growth of population around the world accompanied by a tremendous industrial development result in an enormous demand for global energy consumption. In addition, the evolution of the world towards smart and connected technologies and the daily need for electronic devices such as laptops, smartphones and tablets require highly efficient energy storage systems.[1] Electrochemical double layer capacitors (EDLCs), also called supercapacitors (SCs), are energy storage devices that store energy via adsorption-desorption of ions at the electrode/electrolyte interface. Porous carbons such as activated carbons (ACs) with high specific surface area (more than 1500 $m^2 g^{-1}$) and good electrical and electrochemical properties have been extensively used as electrode material for EDLCs.[1,2]

At the start of the 21st century, the use of nanoporous carbons showed a drastic increase of the capacitive performance.[3] Indeed, a surprising increase in capacitance was achieved by reducing the pore size to the sub-nanometer level (< 1 nm). This discovery has impacted the performance of commercial devices and provided fundamental new insights into the electrical double layer in nanopores. Accordingly, exploring the attractive properties on the nanometric scale to understand the charge storage mechanism of nanoporous carbon-based electrodes is a very effective way to boost the performance of electrochemical capacitors. Many studies have been devoted to investigate the relationship between pore size and ion size, more precisely ion confinement inside nanopores, to describe the ion exchange mechanisms in nanoporous carbon and their influence on the capacitance.[4–6] Reducing the pore size to a size smaller than that of the solvated ions resulted in a partial desolvation and consequently a significant increase in the capacitance.[7]

As capacitive electrodes store charges at the carbon surface, it is of essential to study the influence of the surface chemistry on the specific capacitance, in addition to the porosity. [8] Thermal treatments (TT) under oxygen or under argon are expected to affect the material's surface chemistry, and specific capacitance.[9] For instance, subjecting a carbon surface to a TT under oxygen lead to the introduction of Oxygen Functional Groups (OFGs) such as carboxyl, carbonyl and hydroxyl as a consequence of the gas/active material interaction. The accessibility of the pores may be impeded and/or a pseudocapacitive behavior may be enabled due this effect. [10]Indeed, it

has been proven that OFGs on the material's surface can lead to pseudo-capacitance coming from the reaction from the functional groups and the electrolyte, increasing the global capacitance. [11]

In this work, two different thermal treatments are conducted on commercial ACs aiming at their oxidation or reduction. As the presence of OFGs can alter the surface electronic conductivity, the surface accessibility is also expected to be modified. Such changes can be probed by assessing the heterogeneous electron transfer (HET) rate constants measuring the dynamic effects in the electrode/electrolyte interface.[12,13] As a matter of fact, a higher surface conductivity and a better access to the carbon surface should lead to higher HET. Measurements of the overall (global) and local HET rate constants were conducted. Regarding the global measurement, Nicholson's method was applied for each carbon. [14] However, it is known that the global measurement is affected by the electrode resistance. For instance, the grain-grain contact resistance will make the effective HET lower[13]. It is where local measurement comes into play as it makes the grain-grain resistance less prominent and in turns should lead to a higher effective HET.[15] Scanning electrochemical microscopy (SECM) is a perfect tool for measuring such local rate constants. Global and local measurements of the effective HET were done and compared depending on the TT conditions applied in this work.

Experimental

Materials

In this work, the amount of surface oxygen functional groups on commercially available YP-50F activated carbons (AC), designated was modified through thermal treatments. Air or argon atmosphere was used whether the purpose was to increase or decrease the amount of surface oxygen functional groups, respectively. The appropriate thermal conditions were determined using thermogravimetric analyses (TGA), performed in air and in argon. Accordingly, YP-50F oxidation was done in air at 300 °C for 12h. Then, the powder was kept in the oven until it cooled down to room temperature. YP-50F reduction was carried out under argon atmosphere at 250 °C for 3h. The sample was then cooled to room temperature in argon. In the following, the air oxidized AC was named oAC and the argon reduced AC, rAC.

Materials characterizations

TGA measurements were carried out using a SETARAM TAG 16 by heating the AC up to 800°C with a 5°C min^{-1} heating rate in air for AC oxidation, and in argon atmosphere for AC reduction. Porosity properties of AC materials were investigated using a Micromeritics ASAP2020 instrument, with argon gas as adsorbate. AC materials were outgassed at 200°C under vacuum for 24h. Argon isotherm was measured at 77 K. Specific surface area (SSA) values were determined using Brunauer-Emmett-Taller equation (BET),[16] while pore size distributions (PSD) were obtained from 2D non-local density functional theory (2D-NLDFT) [17] implemented in SAEUIS, from Micrometrics. The surface morphology of all electrodes was characterized by scanning electron microscopy (SEM) VEGA3-Tescan and the chemical composition was analyzed by energy dispersive X-ray spectrometer (EDX) using a JED 2300 detector coupled to SEM.

Electrochemical global measurements

The carbon powders (AC, oAC, and rAC – 90 wt%) were mixed with polyvinylidene fluoride (PVDF) binder (10 wt%) and dispersed in *N*-methyl-2-pyrrolidone (NMP) solvent using an ultrasonic bath. The obtained dispersion was coated by spray gun on stainless steel foil (12 mm in diameter) and dried at 80°C under vacuum for 12 hours. The mass loading of the coating was about 0.4 mg cm^{-2}. The electrochemical tests were carried out in a three-electrode configuration, at room temperature, using a Biologic SP-300 potentiostat. The carbon electrodes were used as working electrode, a Pt foil as counter electrode, and a Ag/AgCl as reference electrode (**Figure 1A**). Cyclic voltammetries (CV) were done from 0 to 0.5 V vs. Ag/AgCl operational potential window (OPW), in a 0.1 M potassium chloride (KCl) electrolyte containing 1 mM ferrocenemethanol (FcMeOH) as an electrochemical probe. Various scan rates (5, 10, 20, 50 and 100 mV s^{-1}) were applied in order to realize kinetic analyses. The CV curves were normalized with respect to the mass of active material. Nicholson's method [14] was used to determine the effective electron transfer rate constant (k_{eff}) for the three carbon electrodes using the CV results.

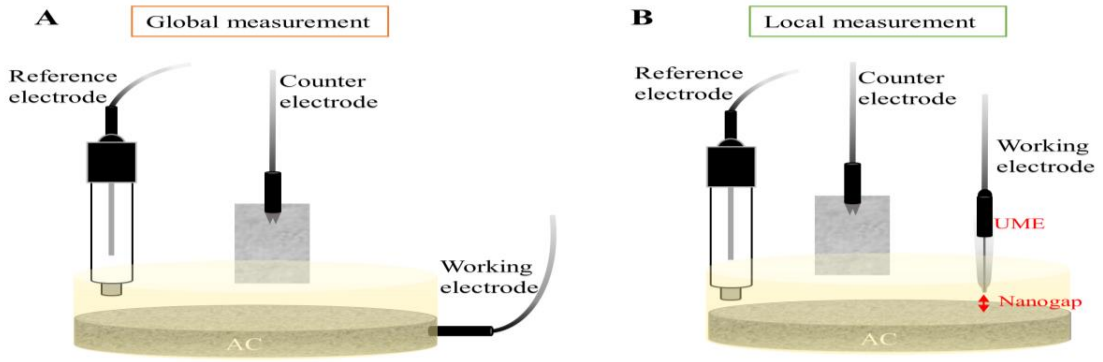

Figure 1: Schematic representation of the experimental setup of (A) global measurements and (B) local measurements. For the global measurements, The AC electrode was used as working electrode, and for the local measurements, a Pt UME was used as working electrode

SECM measurements

SECM experiments were performed under feedback mode with a Biologic SECM instrument (model M470) associated with a SP-300 bipotentiostat. A commercial platinum ultramicroelectrode (Pt-UME with a diameter of ~10 µm) was used together with Pt and Ag/AgCl as working, counter and reference electrodes, respectively (**Figure 1B**). The platinum ultramicroelectrode (Pt-UME) as SECM tip was fixed on an x,y,z-positioning system to control its position over the carbon substrate at the bottom of the SECM cell. All electrodes were emerged in an aqueous electrolyte containing 0.1 M KCl and 1 mM FcMeOH. After each test, the electrolyte was renewed. It is worth noting that for all SECM tests, the carbon substrates were not polarized. The initial approach of the Pt-UME over the substrates was monitored using a video microscope. Initially, it is essential to establish the intermittent contact position between the tip and substrate. This can be achieved by utilizing the piezoelectric mode offered by the Biologic software. In this mode, specific vibration frequencies are associated with different current values, reflecting the distance between the probe and the carbon. The approach of the Pt-UME tip is halted when the physical distance matches the frequency corresponding to the highest calculated current peak observed during intermittent contact. Then, the remaining distance between the substrate and the tip before contact was controlled via the

variation of the feedback current during the approach curve while the tip was biased at 0.5 V vs. Ag/AgCl. The definitive contact, defined by the origin of z-axis, is defined as being the point where the tip current value doubles compared with the bulk. The accuracy of the origin determination was about 5 µm.

SECM-CV curves were measured between the Pt-UME at ~ 200 ± 5 µm (in the bulk solution) and at ~ 1±5 µm from the carbon substrates, in the potential range from 0 to 0.6 V *vs*. Ag/AgCl at a scan rate of 20 mV s^{-1}. The distance standard variation is acquired according to the delimited displacement measured at each experiment,

CV and approach current curves were normalized by the tip current measured in the bulk solution (I_{bulk}).[18]

Results and discussion

In this work, the goal was to study the influence of the oxygen group content on the effective heterogeneous electron charge transfer between a microporous activated carbon and an aqueous electrolyte. To do so, electrochemical characterizations of commercial and thermally treated ACs were performed using conventional CV measurements on the overall AC electrode (global measurement) and using SECM-local approach curve measurements. To determine the proper thermal conditions for oxidation and reduction of the initial activated carbon (YP-50F), TGA analyses were conducted. The results of TGA together with Derivative Thermogravimetry (DTG) of AC, under air and argon atmosphere are shown in Figure 2. In the initial heating range, below 150°C, in both cases, AC exhibits a small weight loss of about 4%, due to the elimination of physiosorbed water molecules. Under air, AC does not experience any weight loss until it gets fully decomposed beyond 550°C (Figure 2A); while only a weight loss of about 11%, around 235°C, is observed for AC heated under argon atmosphere. This weight loss is ascribed to the thermal desorption of surface oxygen groups. [19,20]

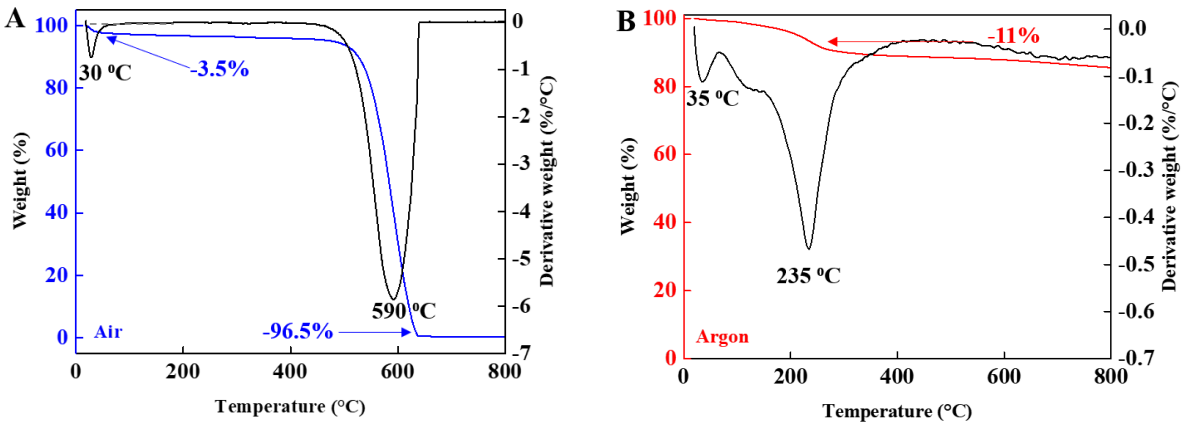

Figure 2: TGA and differential thermal analysis thermograms of the commercial AC powder in (A) air and (B) argon.

Following the TGA analyses, an AC oxidized at 300°C under air for 12 hours, designated as oAC, and an AC reduced at 250°C under argon for 3 hours, designated as rAC, were prepared. Gas sorption analyses were performed on these two carbons and the isotherms are presented in **Figure 3A**. The isotherm of the as-received AC is also shown for comparison. PSDs determined using non-local density functional theory (NL-DFT)[21] are plotted in **Figure 3B**. All the textural properties are summarized in **Table 1**.

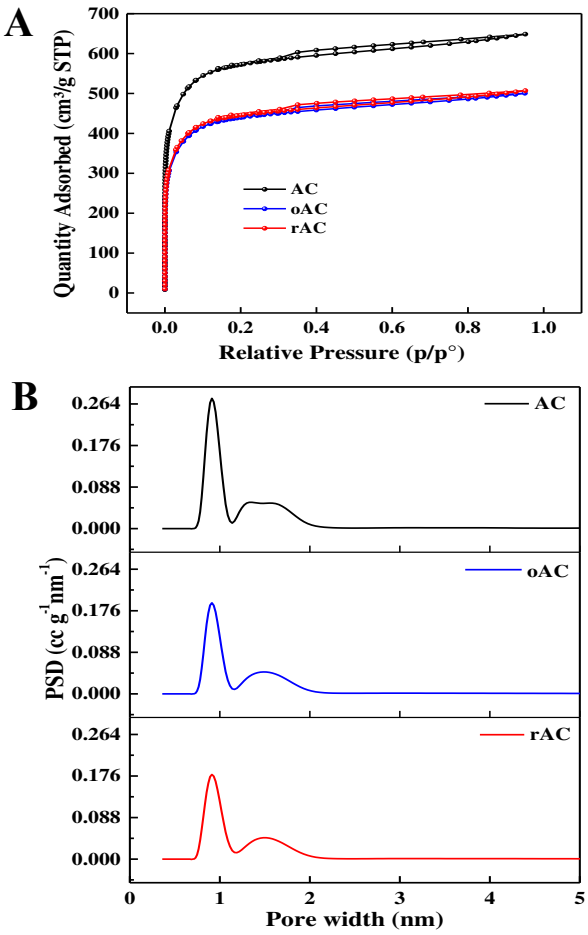

Figure 3: (A) Ar adsorption/desorption isotherms and (B) pore size distributions calculated using NL-DFT for AC, oAC, and rAC.

The isotherm diagrams (**Figure 3A**) exhibit a typical Type I isotherm [22,23], as expected for a microporous carbon. A slight hysteresis is observed and is ascribed to the presence of small amount of mesopores. The untreated AC material presents specific surface area (SSA) values of about 1836 ± 27 m^2 g^{-1} with a total pore volume of 0.99 cm^3 g^{-1} and an average pore size of about 1.2 nm. After oxidation or reduction treatment, the SSA and the total pore volume of both materials decreased by ~25%. However, the overall pore size distribution (PSD) stays the same leading to the same average pore size. Indeed, the three materials showed the same two adsorptions modes, one centered at about 0.9 nm, the other at 1.5 nm. It confirms that the micropore structure was not modified by the oxidation or reduction AC treatment. The SSA decrease for both thermal treated materials could be explained by the blocking of some micropores over the carbon surface thermal pretreatment. For the oxidized activated carbon, there is a small weight increase due the addition of oxygen atoms over its surface, while, in the case of defunctionalized AC, local structural rearrangement in the carbon could explain the decrease of micropore volume.[24]

Table 1: Textural properties of AC, oAC, and rAC powders obtained by Ar adsorption/desorption

Material	S_{BET} (m^2g^{-1})	S_{NLDFT} (m^2g^{-1})	V_t (cm^3g^{-1})	V_{micro} (cm^3g^{-1})	Average pore size (nm)
AC	1836 ± 27	1656	0.99	0.87	1.2
oAC	1332 ± 19	1210	0.71	0.63	1.2
rAC	1348 ± 20	1211	0.72	0.64	1.2

The surface morphology of AC, oAC, and rAC was characterized by SEM analysis. The SEM images and EDX analysis of the films surface are shown in **Figure 4**.

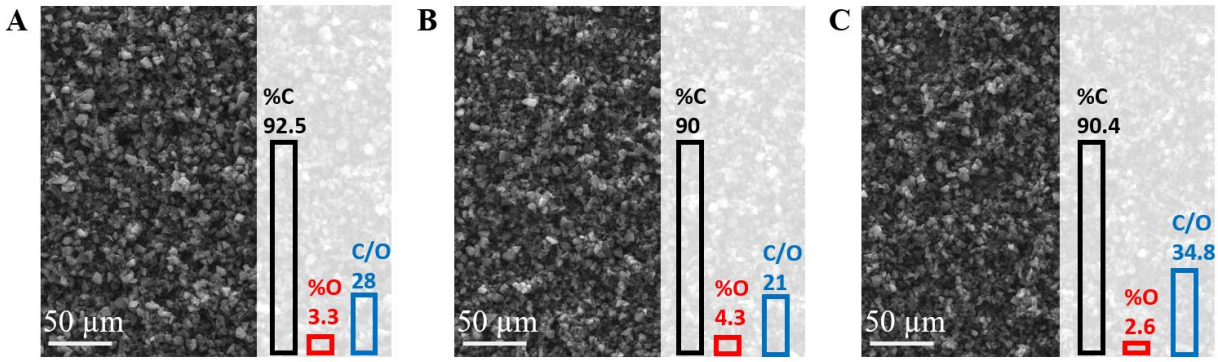

Figure 4: SEM images of (A) AC, (B) oAC, and (C) rAC films. Inset: percentages of oxygen and carbon, and C/O ratio values measured by EDX detector.

According to SEM images, no severe morphology change is observed after the different treatments. EDX analysis shows a slight decrease of the C/O ratio after the thermal oxidation, due the oxygen amount increase, while the opposite is seen after thermal reduction. Those characterization results indicate some surface modifications have occurred during both treatments.

Following Nicholson's paper,[14] the current peak potential separation is dependent on the heterogeneous electron transfer rate constant of the electrode: the larger the current peak potential separation, the lower the HET. In this case, CV curves of AC, oAC, and rAC electrodes, performed in 0.1M KCl containing FcMeOH as mediator at various scan rates, are presented in **Figure 5 (A-C)**. No major changes with oxidation are noticed, as the overall shape and current magnitude are very similar. The results of CVs of the three carbon electrodes are as expected for quasi-reversible redox reactions with a single electron transfer. Going further, the variations of the peak current with the square root of the scan rate are plotted in Figure 5 (D-F) for both the oxidation and the reduction. For all carbons, the peak currents vary linearly, as expected for diffusion-controlled kinetics.[25]

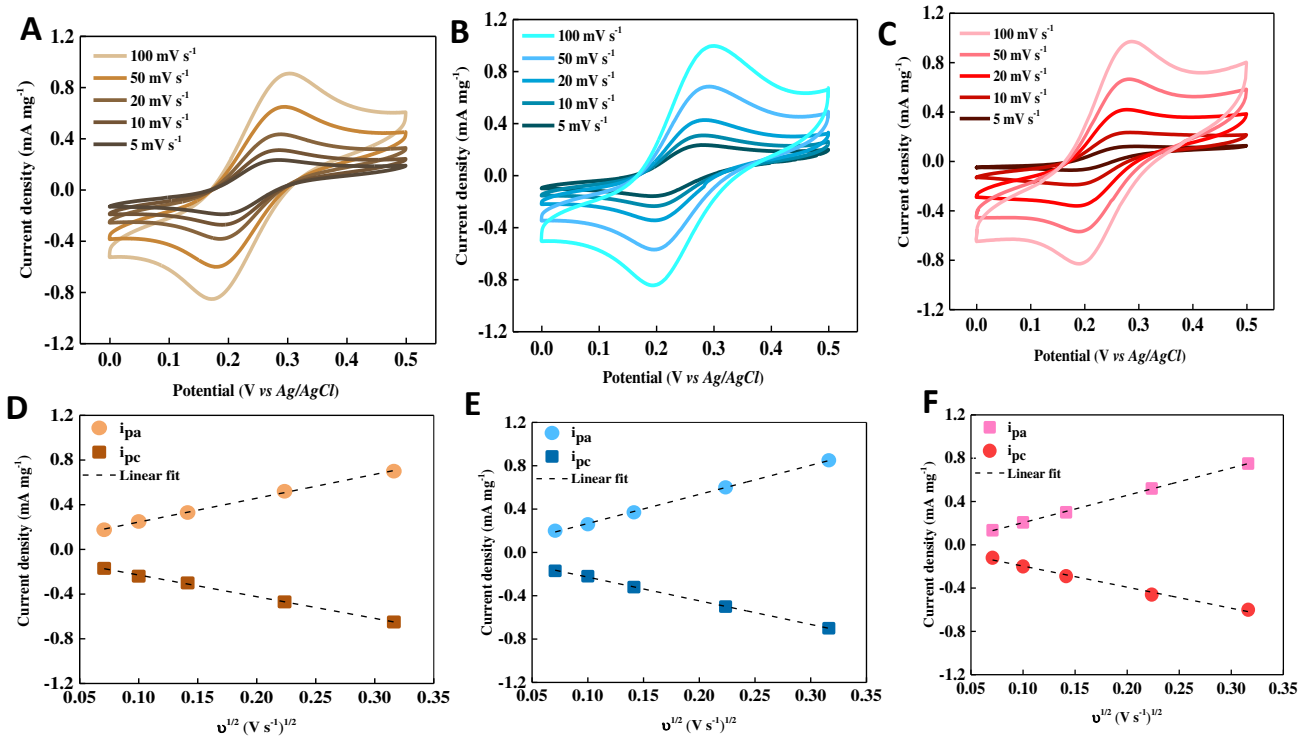

Figure 5: CV curves of (A) AC, (B) oAC, and (C) rAC electrodes performed in 0.1 M KCl aqueous solution containing 1 mM FcMeOH from 0 to 0.5 V vs. Ag/AgCl at various scan rates (5 – 100 mV s-1). Randles-Sevcik plots for (D) AC, (E) oAC, and (F) rAC.

The oxidized AC sample (oAC) exhibits a 20% higher current than the as-received activated carbon (AC) which could be linked to the presence of higher amount of oxygen groups adding a pseudo capacitive contribution in the material. For the carbon having a lower oxygen content (rAC), the current density is around 10% lower, especially at slower scan rates. The influence of oxygen groups content is more marked when comparing the peak-to-peak separation ($\Delta_{Ep} = |E_{pa} - E_{pc}|$) values (**Figure 6A**).

Starting with the same mass loadings for all the electrodes (0.15 mg/cm^2), the cycling voltammetry in presence of no redox mediator at the electrolyte, presented a no redox peaks profile. The observed peaks can be attributed to the interaction between the electrode and the redox mediator in the

electrolyte. In the presence of FcMeOH dissolved in the electrolyte, the oxidation treatment of AC leads to a decrease of Δ_{Ep} at different scan rates, while the reduction of AC shows a distinctly different electrochemical behavior. For the lowest scan rates, rAC electrode exhibits higher Δ_{Ep} values, and at faster scan rates, lower Δ_{Ep} values compared to AC electrode. The Δ_{Ep} value variation for both different treatments are due to the different interaction between the carbon surface and the electrolyte's redox mediator, since different functional groups are reacting for both treatments. [25] The Δ_{Ep} values were used to calculate the charge transfer rate constant (k_{eff}) using the following equation[14]:

$$k_{eff} = (DnFv/RT)^{1/2}\Psi \quad (1)$$

where Ψ is the kinetic parameter related to the Δ_{Ep} value (Table S1) [26], *D* is the diffusion coefficient of the redox mediator ($cm^2\ s^{-1}$), calculated from Randles-Sevcick equation [13], *n* is the number of the electrons involved in the redox reaction, *F* is the Faraday constant (96 485 C mol^{-1}), *v* is the scan rate (V s^{-1}), *R* is the gas constant (8.3145 J mol^{-1} K^{-1}),and *T* is the temperature (K). The calculated k_{eff} values of AC, oAC, and rAC electrodes at different scan rates, are reported in **Figure 6B**.

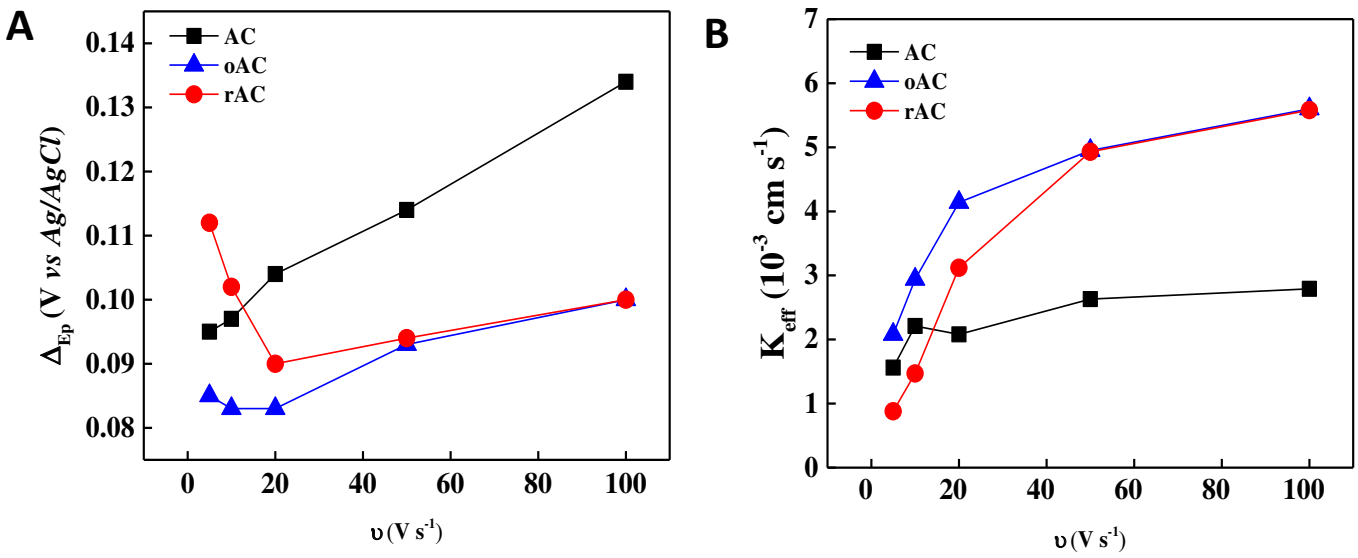

Figure 6: (A) Peak-to-peak separation (Δ^{Ep}) and (B) charge transfer constant (k_{eff}) values for AC, oAC, and rAC at different scan rates (5 – 100 mV s^{-1}) calculated by eq 1.

In figure 6B are presented the effective HET rate constants for the three carbons at different scan rates. As observed, the effective HET is mostly constant for the non-treated AC while it increases with scan rate for the other two carbons. Between scan rates of 50 mV/s and 100 mV/s, the absolute values of the HET for both treated carbons exhibit an approximate twofold increase and a similar behavior. For the lower scan rates, on the other hand, the charge transfer constant is approximately twice as important for oAC than for rAC. This characteristic, first observed by Reinmuth [27] and further explained by Klingler and Kochi [28], support a k_{eff} behavior change with different scan rates is due a lower reversibility. Then, as the sweep rate increases, the peak separation potential slightly increases, while the i_p^a / i_p^c remains constant for every ν.

Based on the eq 2 provided by Nicholson and Shain [29] as an alternative method for the evaluation of k_{eff}, expressed in eq 1, the calculated value of the effective constant will increase regularly with the sweep rate, that influences Ψ for reversible reactions However, it will eventually reach a point where further increases in the scan rate will offset the complementary changes in the peak separation and in this case, k_{eff} will become independent of the peak separation and as consequence,

the scan rate._Kingler and Kochi also confirmed that the simulated k_{eff} values_evaluated by Nicholson's method in eq 1 and eq 2 are the same under the same experimental conditions.

$$k(E) = 2.18\,[\frac{D\beta nF\upsilon}{RT}]^{\frac{1}{2}} \exp[\frac{\beta nF}{RT}(E - E^{\circ})] \quad (2)$$

Where D is the diffusion coefficient, β is the transfer coefficient for the electrode process, describing the degree of reversibility of a redox reaction between 0 and 1, calculated by independent methods [28], n is the number of electrons transferred in the rate-limiting step, F is the Faraday constant, E is the electrode's potential between the electrode and electrolyte solution and E° denotes the standard potential, measured under standard conditions, used as reference point.

Local measurements

SECM measurements were performed to investigate the local influence of oxygen groups on the heterogenous electron transfer rate at activated carbon. Cyclic voltammograms measured using a Pt-UME over the AC, oAC, and rAC substrates, are shown in **Figure 7**.

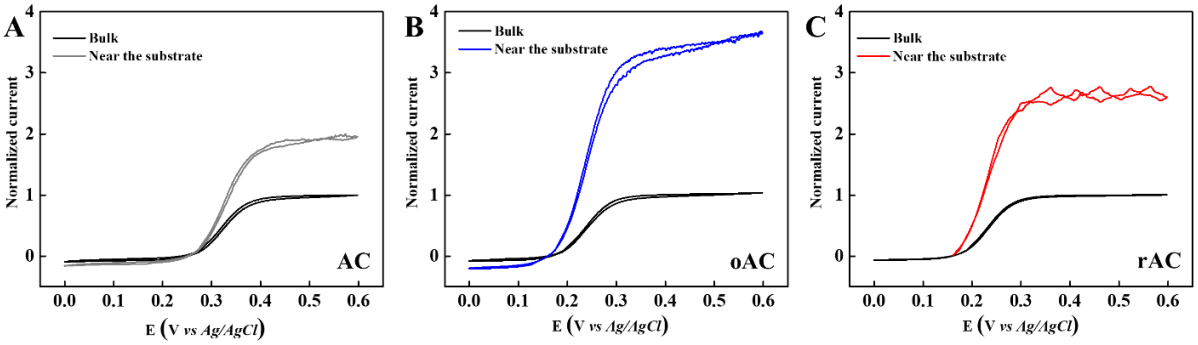

Figure 7: CV curves measured by Pt-UME in the bulk (~200 µm) and near (~1 µm) (A) AC, (B) oAC, and (C) rAC electrodes, in an 0.1 M KCl aqueous solution containing 1 mM FcMeOH from 0 to 0.6 V vs. Ag/AgCl at a scan rate of 20 mV s^{-1}.

The CV current was normalized with respect to the tip current measured in the bulk of the electrolyte, $i_{T,\infty}$. As observed, the voltammograms measured at about 200 µm from the carbon substrates are sigmoidal, without hysteresis: a steady-state response independent of v is reached, as under these experimental conditions spherical diffusion prevails.[30] Furthermore, these curves have the same current variation at the bulk, as the Pt-UME is far enough from the substrate to avoid any feedback.[31] When the tip is in the vicinity of the substrate (~1 µm), the voltammograms exhibits a higher current compared to that measured in the bulk, showing a positive feedback, for all the carbons studied. Indeed, as the three carbons tested are conductive, they allow for the regeneration of the mediator, causing an increase in the ultramicroelectrode (UME) current. As it is assumed that the diffusion coefficient is the same for the oxidized and the reduced forms of the electrochemical mediator, the current increase is likely related to the adsorption and regeneration of the mediator at the carbon surface.[13] Even though the current increases for all the carbons, different current amplification is found depending on the carbon tested. For the as-received AC substrate the current increased by about 2 times at the tip/substrate contact level, meanwhile, for oAC and rAC substrates, the current increased by about 3.5 and 2.75 times respectively, with respect to the CV current measured in the bulk electrolyte. These results confirmed the significant influence of the carbon surface state on the effective HET rate. In the experimental conditions chosen in this work, it turns out that both thermal treatments lead to higher current so higher HET rate.

In order to calculate the HET rate constant (k_{eff}), the SECM approach curves were performed by approaching the Pt-UME toward the carbon substrates in feedback mode under the same electrolyte as the global measurements. The tip was biased at a potential of 0.5 V *vs.* Ag/AgCl to oxidize FcMeOH while approaching the surface of the substrates and measuring the current. All along the measurement, the carbon being tested are kept at open circuit potential. The approach curves of Pt-UME over AC, oAC, and rAC substrates are reported in **Figure 8**.

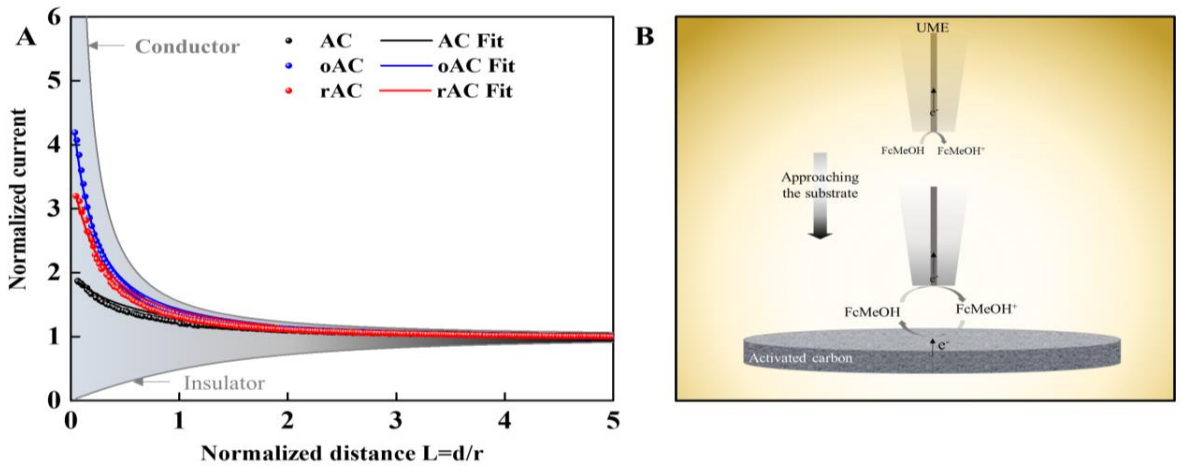

Figure 8: Approach curves performed with Pt-UME (10 um in diameter) on AC, oAC, and rAC, in 0.1 M KCl solution containing 1 mM FcMeOH. The Pt-UME was biased at 0.5 V vs. Ag/AgCl and positioned at an initial distance of about 200 µm from the carbon electrodes.

As shown in **figure 8**, for normalized distances L higher than 2, the current remains stable and does not depend on the carbon surface state. It is considered that there is no tip-substrate interaction. Differently, for tip distances from the surface lower than 2, the current increases in accordance with a positive feedback, as expected for conductive samples, it is related to the oxidation of Fc(MeOH) at the Pt-UME.[32]

The experimental approach curves were fitted accordingly with the method described by Bard and Mirking [28,31] to determine the HET rate constant, k_{eff}, values. According to the fitting process, the normalized rate constant, K, was determined, then, k_{eff} was calculated using the following equation[33]:

$$K = \frac{k_{eff} r_T}{D} \quad (3)$$

where r_T is the radius of Pt-UME (~5 µm) and D is the diffusion coefficient of FcMeOH. The obtained results are reported in **Table 3** as it is compared with the local values for AC, oAC and rAC. Among the three carbons, the oAC has demonstrated the higher k_{eff} value, 8.3 10^{-2} cm s^{-1}, compared to that of AC and rAC, which present k_{eff} respectively a k_{eff} of about 3.4 10^{-2} cm s^{-1}, and 6.3 10^{-2} cm s^{-1}, agreeing with the global HET order calculated by Nicholson's method (Figure 6B). Such findings show that carbon surface state plays a key role in the electrochemical charge transfer kinetic. Although the SSA of oAC and rAC are lower than that of AC, these two carbons exhibit a higher HET. This result may be linked to local carbon's electronic structure that is highly likely to change with the amount of surface oxygen functional groups.[11] Table 2 shows the k_{eff} value in function of their respective SSA, understanding the influence of the porosity at the HET in a local way.

Table 2: Normalized local HET by their Specific Surface Area

Electrode	**k_{eff}/SSA (g m^{-1} s^{-1})**
AC	1.85 10^{-7}
oAC	6.23 10^{-7}
rAC	4.67 10^{-7}

The resolution of an *in situ* and local measurement versus a global measurement can be noticed trough the different effective constants for the same material versus the "averaged" response in the global[32] way, being seen as a limitation, as the value may be lower because of a lower electron transport throughout the AC film. Comparing the HET values obtained by the micro and macro electrode analysis, we can see that the order of each material's reactivity is kept, but the absolute value is increased by one order of magnitude with SECM measurements. Comparing local and global effective HET may bring information about the electron transport within the AC film—a large $k_{eff\ local}/k_{eff\ global}$ may indicate the electron transport through the AC film is impeded by a higher

grain-grain electrical contact resistance. **Table 3** gives the calculated k_{eff} through the local and global technique for comparison, their ratios have been also calculated.

Table 3: k_{eff} values calculated using CV curves of Nicholson's method for 20 mV s^{-1} and SECM approach curves.

Electrode	k_{eff} **(cm** s^{-1}**)**		$\frac{k_{efflocal}}{k_{effglobal}}$
	Global measurements (CV)	**Local measurements (SECM-approach curve)**	
AC	2.1 10^{-3}	3.4 10^{-2}	16
oAC	4.1 10^{-3}	8.6 10^{-2}	20
rAC	3.1 10^{-3}	6.3 10^{-2}	20

The oAC presents the highest HET in both analysis and for all scan rates, consistent with the higher specific current during the electrochemical tests and confirming the increase of reactivity and capacity through the addition of oxygen functional groups in the carbon's surface. For the rAC, the HET increases in relation to AC in higher scan rates (50 mV s^{-1} and 100 mV s^{-1}), as an evidence that the thermal treatment for the AC improve its performance and kinetics. Besides, the HET ratios show the TT lead to higher ratio that may suggest that the contact resistance has been affected by the TT and the change of surface chemistry.

Conclusions

Local and global measurement were applied on an as-received activated carbon and two different thermal treated ACs (oxidized oAC and reduced rAC) in order to investigate the effective HET rate constants showing the reactivity of the electrode surface for a given electrolyte. For all three cases, the sigmoidal CV shape obtained during macroelectrode's cycling shows a reversible reaction in which the oAC presented the highest current and highest charge transfer constant ($8.6\ 10^{-2}$ cm s^{-1}) followed by rAC ($6.3\ 10^{-2}$ cm s^{-1}) and AC ($3.4\ 10^{-2}$ cm s^{-1}), demonstrating that a thermal treatment under air and argon might improve carbon's capacitance. The effective HET rate constants measured from SECM at the local scale were always higher than the one measured for the overall AC electrode, for the AC tested. A higher difference was observed for both TT AC that may be due to the modification of the surface chemistry after TT, which in turns leads to a higher grain-grain contact resistance.

Acknowledgements

This project has received funding from the European Research Council (ERC) under the European Union's Horizon 2020 research and innovation program (grant agreement no. 714581) and ANR SPICS program (ANR-19-CE05-0035).

References

(1) Simon, P.; Gogotsi, Y. Perspectives for Electrochemical Capacitors and Related Devices. *Nat. Mater.* **2020**, *19* (11), 1151–1163. https://doi.org/10.1038/s41563-020-0747-z.

(2) Shao, H.; Wu, Y.-C.; Lin, Z.; Taberna, P.-L.; Simon, P. Nanoporous Carbon for Electrochemical Capacitive Energy Storage. *Chemical Society Reviews* **2020**, *49* (10), 3005–3039. https://doi.org/10.1039/D0CS00059K.

(3) Chmiola, J.; Yushin, G.; Gogotsi, Y.; Portet, C.; Simon, P.; Taberna, P. L. Anomalous Increase in Carbon Capacitance at Pore Sizes Less Than 1 Nanometer. *Science* **2006**, *313* (5794), 1760–1763. https://doi.org/10.1126/science.1132195.

(4) Chmiola, J.; Largeot, C.; Taberna, P.-L.; Simon, P.; Gogotsi, Y. Desolvation of Ions in Subnanometer Pores and Its Effect on Capacitance and Double-Layer Theory. *Angewandte Chemie International Edition* **2008**, *47* (18), 3392–3395. https://doi.org/10.1002/anie.200704894.

(5) Merlet, C.; Rotenberg, B.; Madden, P. A.; Taberna, P.-L.; Simon, P.; Gogotsi, Y.; Salanne, M. On the Molecular Origin of Supercapacitance in Nanoporous Carbon Electrodes. *Nature Mater* **2012**, *11* (4), 306–310. https://doi.org/10.1038/nmat3260.

(6) Merlet, C.; Pe´an, C.; Rotenberg, B.; Madden, P. A.; Daffos, B.; Taberna, P. L.; Simon, P.; Salanne, M. Highly Confined Ions Store Charge More Efficiently in Supercapacitors. *Nature Communications* **2013**. https://doi.org/10.1038/ncomms3701.

(7) He, Y.; Zhang, Y.; Li, X.; Lv, Z.; Wang, X.; Liu, Z.; Huang, X. Capacitive Mechanism of Oxygen Functional Groups on Carbon Surface in Supercapacitors. *Electrochimica Acta* **2018**, *20*, 618–625. https://doi.org/10.1016/j.electacta.2018.06.103.

(8) Qu, D.; Shi, H. Studies of Activated Carbons Used in Double-Layer Capacitors. *Journal of Power Sources* **1998**, *74*, 99–107.

(9) Yumak, T. Effect of Synthesis Methods on the Surface and Electrochemical Characteristics of Metal Oxide/Activated Carbon Composites for Supercapacitor Applications. *Applied Surface Science* **2019**.

(10) Dastgheib, S. A.; Karanfil, T. Adsorption of Oxygen by Heat-Treated Granular and FIbrous Activated Carbons. *Journal of Colloid and Interface Science* **2004**, *274*.

(11) Chen, Y.; Zhang, Z.; Huang, Z.; Zhang. Effects of Oxygen-Containing Functional Groups on the Supercapacitor Performance of Incompletely Reduced Graphene Oxides. *International journal of Hydrogen Energy* **2017**, *45*.

(12) Fawcet, W. R.; Opallo, M. The Kinetics of Heterogeneous Electron Transfer Reaction in Polar Solvents. *Angewandte Chemie International Edition in English* **1994**, *33*, 2131–2143. https://doi.org/10.1002/anie.199421311.

(13) Park, J.; Kumar, V.; Wang, X.; Lee, P. S.; Kim, W. Investigation of Charge Transfer Kinetics at Carbon/Hydroquinone Interfaces for Redox-Active-Electrolyte Supercapacitors. *ACS Appl. Mater. Interfaces* **2017**.

(14) Nicholson, R. S. Theory and Application of Cyclic Voltammetry for Measurement of Electrode Reaction Kinetics. **1965**, *37*.

(15) Gao, Q.; Tsai, W.-Y.; Balke, N. In Situ and Operando Force-Based Atomic Force Microscopy for Probing Local Functionality in Energy Storage Materials. *Electrochemical Science Advances* **2021**.

(16) Brunauer, S. P. H.; Emmett, P. H.; Teller, E. Adsorption of Gases in Multimolecular Layers. *Journal of the American Chemical Society* **1938**, *60*, 309–319.

(17) Seaton, N. A.; Walton, J. P. R. B.; quirke, N. A New Analysis Method for the Determination of the Pore Size Distribution of Porous Carbons from Nitrogen Adsorption Measurements. *Carbon 27*, 853–861.

(18) Kai, T.; G. Zoski, C.; Bard, A. J. Scanning Electrochemical Microscopy at the Nanometer Level. *Chemical Communications* **2018**, *54*. https://doi.org/doi.org/10.1039/C7CC09777H.

(19) McAllister, M. J.; Li, J.-L.; Adamson, D. H.; Schniepp, H. C.; Abdala, A. A.; Liu, J.; Herrera-Alonso, M.; Milius, D. L.; Car, R.; Prud'homme, R. K.; Aksay, I. A. Single Sheet Functionalized Graphene by Oxidation and Thermal Expansion of Graphite. *Chemical Materials* **2007**, *19*, 4396–4404.

(20) Kariim, I.; Abdulkareem, A. S.; Abubakre, O. K. Development and Characterization of MWCNTs from Activated Carbon as Adsorbent for Metronidazole and Levofloxacin Sorption from Pharmaceutical Wastewater: Kinetics, Isotherms and Thermodynamic Studies. *Scientific African* **2020**, *7*.

(21) Tarazona, P. Free-Energy Density Functional for Hard Spheres. *Physical Review* **1985**, *31* (4).

(22) Lykiema, J.; Sing, K. S. W.; Haber, J.; Kerker, M.; Wolfram, E.; Block, J. H.; Churaev, N. V.; Everett, D. H.; Hansen, R. S.; Haul, R. A. W.; Hightower, J. W.; Hunter, R. J. Reporting Physisorption Data for Gas/Solid Systems with Special Reference to the Determination of Surface Area and Porosity. *Pure and Applied Chemistry* **1984**.

(23) Donohue, M. D.; Aranovich, G. L. Classification of Gibbs Adsorption Isotherms. *Advances in Colloid and Interface Science* **1998**, *76–77*.

(24) Bleda-Martınez, M. J.; Lozano-Castello, D.; Morallón, E.; Cazorla-Amorós, D.; Linares-Solano, A. Chemical and Electrochemical Characterization of Porous Carbon Materials. *Carbon* **2006**, *44*.

(25) Neudeck, A.; Dittrich, J. The Determination of Diffusion Coefficients and Rate Constants from the Dependence of the Peak Separation and Peak Current on the Scan Rate of Cyclic Voltammograms at Micro-Cylindrical Electrodes. *Journal of Electroanalytical Chemistry* **1991**, 37–59.

(26) Nioradze, N.; Kim, J.; Amemiya, S. Quasi-Steady-State Voltammetry of Rapid Electron Transfer Reactions at the Macroscopic Substrate of the Scanning Electrochemical Microscope. *Analytical Chemistry* **2011**.

(27) Reinmuth, W. H. Inversible Systems in Stationary Electrode Polarography. *Analytical Chemistry* **1960**.

(28) Klingler, R. J.; Kochi, J. K. Electron-Transfer Kinetics from Cyclic Voltammetry. Quantitative Description of Electrochemical Reversibility. *The Journal of Physical Chemistry* **1981**, 1731–1741.

(29) Nicholson, R. S.; Shain, I. Experimental Verification of an ECE Mechanism for the Reduction of P-Nitrosophenol, Using Stationary Stationary Electrode Polarography. *Analytical Chemistry* **1965**.

(30) Fu, Q.; Yang, F.; Bao, X. Interface-Confined Oxide Nanostructures for Catalytic Oxidation Reactions. *Accounts of chemical research* **2013**, *46*, 1692–1701.

(31) Lee, Y.; Amemiya, S.; Bard, A. J. Scanning Electrochemical Microscopy. 41. Theory and Characterization of Ring Electrodes. *Analytical Chemistry* **2001**, 2261–2267.

(32) Lindsey, G.; Abercrombie, S.; Denuault, G.; Daniele, S. Scanning Electrochemical Microscopy: Approach Curves for Sphere-Cap Scanning Electrochemical Microscopy Tips. **2007** 2952–295

(33) Wei, C.; Bard, A. J.; Mirkin, M. V. Scanning Electrochemical Microscopy: Application of SECM to the Study of Charge Transfer Processes at the Liquid/Liquid Interface. *Journal of Physical Chemistry* **1995**, *99*, 1603–16042.